

Fig 1

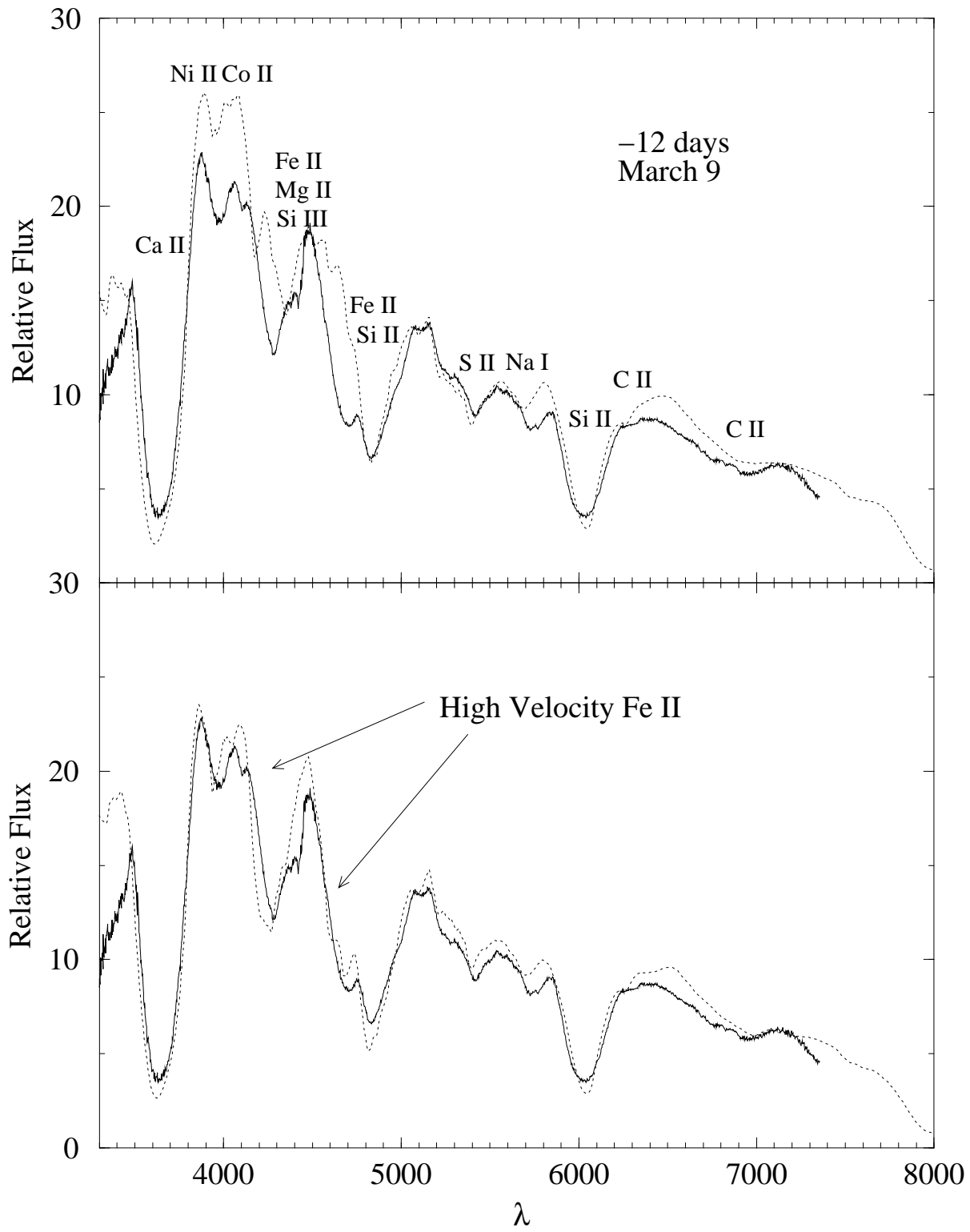


TABLE 1  
FITTING PARAMETERS FOR FIGURE 1

ion	$\lambda$	$\tau$	$v_{min}$	$v_{max}$	$T_{exc}$
Ca II	3934	500	...	40	10
Si II	6347	7	...	27	10
C II	4267	0.03	...	30	10
Ni II	4067	0.07	...	19	10
Co II	4161	0.1	...	19	10
Fe II	5018	0.8	...	17	10
S II	5454	3	...	15	10
Fe III	3013	1.2	18	19	10
Si III	4553	1	...	15	10
Mg II	4481	1	...	17	10
Na I	5890	0.3	...	24	10
Fe II	5018	1.5	22	29	10

Fig 2

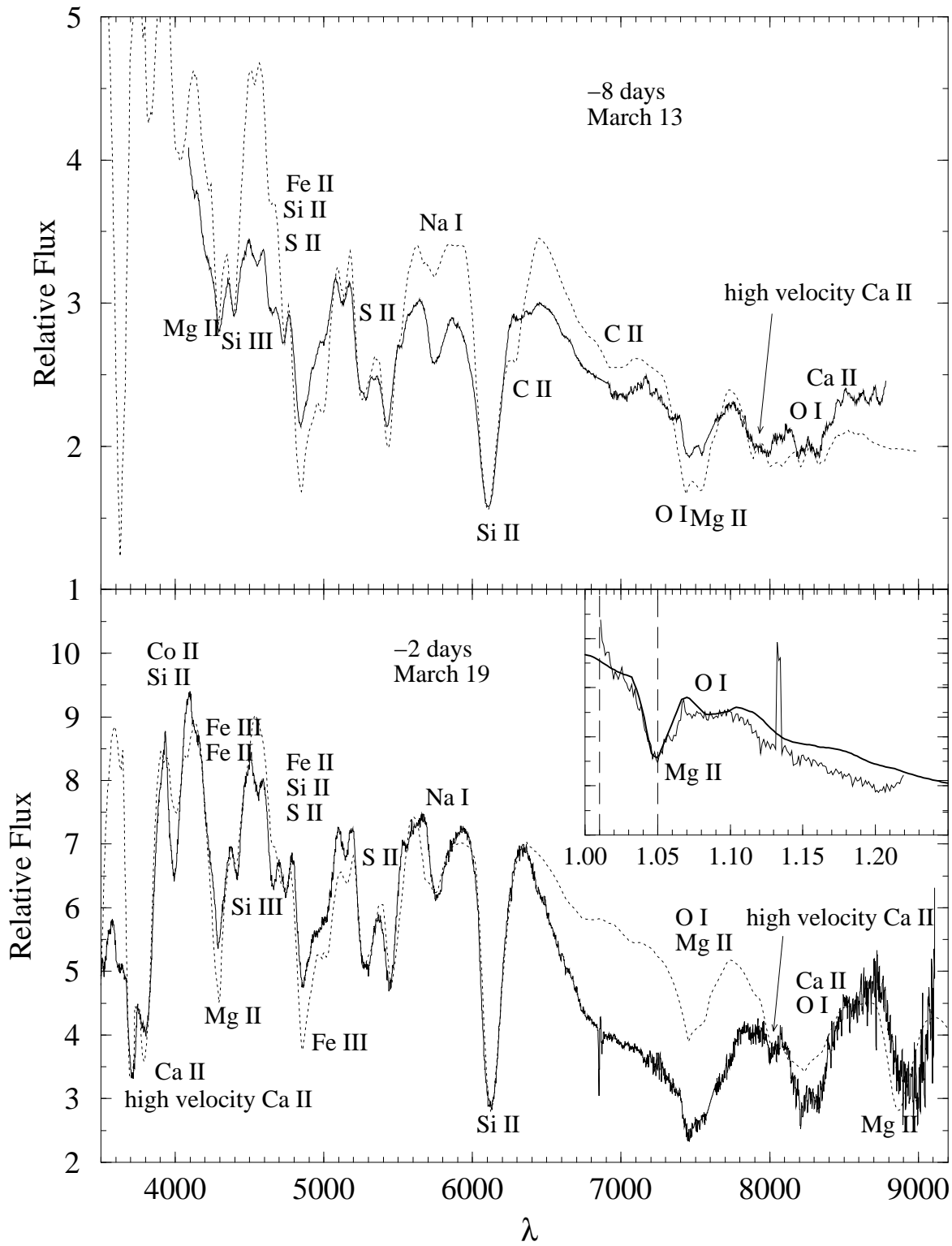


TABLE 2  
FITTING PARAMETERS FOR FIGURE 2 (TOP)

ion	$\lambda$	$\tau$	$v_{min}$	$v_{max}$	$T_{exc}$
Ca II	3934	15	...	13	10
Ca II	3934	3	25	40	10
Si II	6347	1.2	...	20	15
C II	4267	0.02	14	30	10
O I	7772	0.35	14	20	10
Fe II	5018	1.2	...	16	10
S II	5454	2	...	14.5	15
Fe III	3013	0.4	14	20	10
Si III	4553	2.8	...	14	10
Mg II	4481	1	14	17	10
Na I	5890	0.2	...	20	10
Fe II	5018	0.2	20	25	10

Fig 3

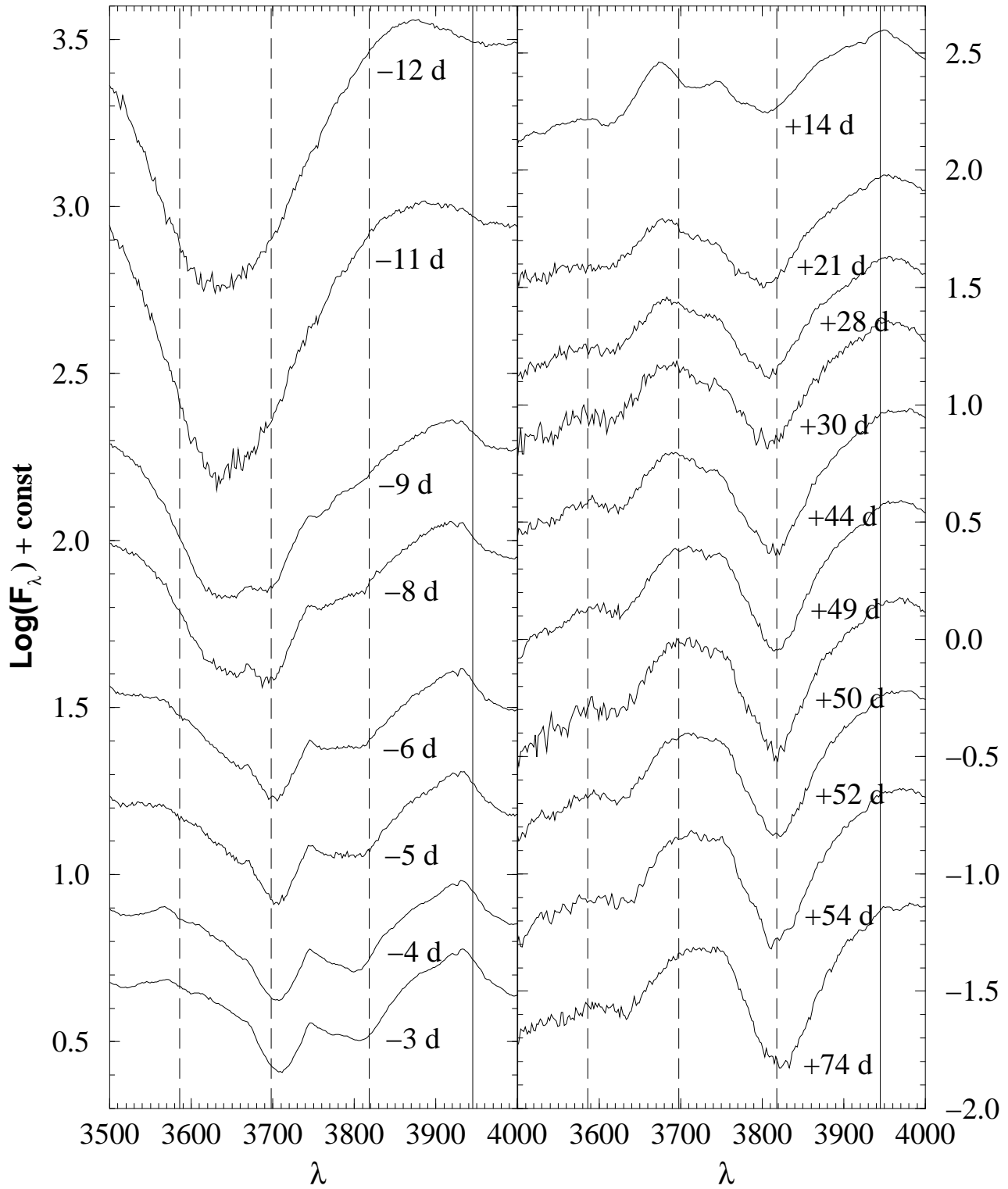


TABLE 3  
FITTING PARAMETERS FOR FIGURE 2 (BOTTOM)

ion	$\lambda$	$\tau$	$v_{min}$	$v_{max}$	$T_{exc}$
Ca II	3934	8	...	16	10
Ca II	3934	2.5	20	23	10
O I	7772	0.3	13	30	10
Si II	6347	1.7	...	16	10
Ni II	4067	0.2	...	20	10
Co II	4161	0.5	...	20	10
Fe II	5018	0.8	...	13	10
S II	5454	1.5	...	13	10
Fe III	3013	0.3	...	20	10
Si III	4553	0.3	...	14	10
Mg II	4481	0.6	13	17	10
Na I	5890	0.3	...	17	10
Fe II	5018	0.3	20	25	10

# On the High–Velocity Ejecta of the Type Ia Supernova 1994D

Kazuhito Hatano<sup>1</sup>, David Branch<sup>1</sup>, Adam Fisher<sup>1</sup>, E. Baron<sup>1</sup>, and A. V. Filippenko<sup>2</sup>

Received \_\_\_\_\_; accepted \_\_\_\_\_

arXiv:astro-ph/9903333v2 27 Jun 1999

---

<sup>1</sup>Department of Physics and Astronomy, University of Oklahoma, Norman, Oklahoma 73019, USA

<sup>2</sup>Department of Astronomy, University of California, Berkeley, CA 94720–3411

## ABSTRACT

Synthetic spectra generated with the parameterized supernova synthetic-spectrum code SYNOW are compared to spectra of the Type Ia SN 1994D that were obtained before the time of maximum brightness. Evidence is found for the presence of two-component Fe II and Ca II features, forming in high velocity ( $\geq 20,000 \text{ km s}^{-1}$ ) and lower velocity ( $\leq 16,000 \text{ km s}^{-1}$ ) matter. Possible interpretations of these spectral splits, and implications for using early-time spectra of SNe Ia to probe the metallicity of the progenitor white dwarf and the nature of the nuclear burning front in the outer layers of the explosion, are discussed.

*Subject headings:* radiative transfer – supernovae: general – supernovae: individual: SN 1994D.



## 1. Introduction

SN 1994D, in the Virgo cluster galaxy NGC 4526, was discovered two weeks before the time of maximum brightness (Treffers et al. 1994) and became the best observed Type Ia supernova (Richmond et al. 1995; Patat et al. 1996; Meikle et al. 1996; Vacca & Leibundgut 1996; Filippenko 1997a,b). The high-quality early-time spectra of SN 1994D, beginning 12 days before maximum brightness, present us with an opportunity to look for spectral lines produced by “primordial” matter, i.e., heavy elements that were already present in the progenitor white dwarf before it exploded, as well as to probe the nature of the nuclear burning front in the outer layers of the ejected matter.

In this paper we report some results of a “direct analysis” of photospheric-phase spectra of SN 1994D using the parameterized supernova spectrum-synthesis code SYNOW (Fisher et al. 1997, 1999; Millard et al. 1999; Fisher 1999). Here we concentrate mainly on spectra obtained before maximum light. An analysis of the post-maximum photospheric-phase spectra will be presented in another paper.

## 2. Previous Studies of SN 1994D Spectra

Numerous optical spectra of SN 1994D have been published by Patat et al. (1996), Meikle et al. (1996), and Filippenko (1997a,b). Patat et al. emphasized that in spite of some photometric peculiarities such as being unusually blue, SN 1994D had the spectral evolution of a normal SN Ia, especially like that of SN 1992A (Kirshner et al. 1993). Meikle et al. also emphasized the spectral resemblance to SN 1992A, and presented some near-infrared spectra.

Höflich (1995) calculated light curves and detailed non-local-thermodynamic-equilibrium (NLTE) spectra for a series of delayed-detonation hydrodynamical models and

found that one particular model — M36, which contained  $0.60 M_{\odot}$  of freshly synthesized  $^{56}\text{Ni}$  — gave a satisfactory representation of the light curves and spectra of SN 1994D. Synthetic spectra for model M36 were compared to observed SN 1994D spectra at epochs of  $-10, -5, 0, 11,$  and  $14$  days. (We cite spectrum epochs in days with respect to the date of maximum brightness in the  $B$  band, 1994 March 21 UT [Richmond et al. 1995].) The good agreement between the calculated and observed spectra and light curves indicated that the composition structure of SN 1994D resembled that of model M36 at least in a general way.

Patat et al. (1996) compared their observed  $-4$  day spectrum to a Monte Carlo synthetic spectrum calculated for the carbon–deflagration model W7 (Nomoto, Thielemann, & Yokoi 1994), which has a composition in its outer layers that differs significantly from model that of M36. This calculated spectrum also agreed reasonably well with the observed spectrum.

Meikle et al. (1996) concentrated on identifying an infrared P Cygni feature that appeared in their pre–maximum–light spectra. They considered He I  $\lambda 10830$  and Mg II  $\lambda 10926$ , and found that in parameterized synthetic spectra either transition could be made to give a reasonable fit, but then other transitions of these ions produced discrepancies elsewhere in the spectrum. Mazzali & Lucy (1998) also focused on identifying the infrared feature. They found that either He I or Mg II could be made to give a reasonable fit, but that neither could explain the rapid disappearance of the observed feature after the time of maximum brightness. Wheeler et al. (1998) favored the Mg II identification and concluded that within the context of delayed–detonation models the feature blueshift provides a sensitive diagnostic of the density at which the deflagration switches to a detonation.

### 3. Spectrum Synthesis Procedure

We have been using the fast, parameterized, supernova spectrum–synthesis code SYNOW to make a direct analysis of photospheric–phase spectra of SN 1994D. The goal has been to establish line identifications and intervals of ejection velocity within which the presence of lines of various ions are detected, without adopting any particular hydrodynamical model. In our work on SN 1994D we have made use of the results of Hatano et al. (1999), who presented plots of LTE Sobolev line optical depths versus temperature for six different compositions that might be expected to be encountered in supernovae, and also presented SYNOW optical spectra for 45 individual ions that can be regarded as candidates for producing identifiable spectral features in supernovae. (Electronic data for the Hatano et al. [1999] paper, now extended to include the near infrared, can be obtained at [www.nhn.ou.edu/~baron/papers.html](http://www.nhn.ou.edu/~baron/papers.html)).

For comparison with each observed spectrum, we have calculated many synthetic spectra with various values of the fitting parameters. These include  $T_{bb}$ , the temperature of the underlying blackbody continuum;  $T_{exc}$ , the excitation temperature; and  $v_{phot}$ , the velocity of matter at the photosphere. For each ion that is introduced, the optical depth of a reference line also is a fitting parameter, with the optical depths of the other lines of the ion being calculated for LTE excitation at  $T_{exc}$ . We also can introduce restrictions on the velocity interval within which each ion is present; when the minimum velocity assigned to an ion is greater than the velocity at the photosphere, the line is said to be detached from the photosphere. The radial dependence of all of the line optical depths is taken to be exponential with  $e$ –folding velocity  $v_e = 3000 \text{ km s}^{-1}$ , and the line source function is taken to be that of resonance scattering. All of the adopted fitting parameters are given in Tables 1–3. The most interesting parameters are  $v_{phot}$ , which as expected is found to decrease with time, and the individual ion velocity restrictions, which constrain the composition structure.

## 4. Results

### 4.1. Twelve Days Before Maximum

The  $-12$  day observed spectrum appears in both the upper and lower panels of Figure 1. The upper panel also contains a SYNOW synthetic spectrum based on what could be called the conventional interpretation of early-time SN Ia spectra (Filippenko 1997 and references therein). The adopted value of  $v_{phot}$  is  $15,000 \text{ km s}^{-1}$ . The ions that are certainly required to account for certain spectral features are Ca II, Si II, S II, and Fe II. In an attempt to improve the fit we also have introduced weaker contributions from C II, Na I, Mg II, Si III, Fe III, Co II, and Ni II, some with minimum and maximum velocities as listed in Table 1. (Ions for which no minimum velocity is listed are undetached, i.e., their listed optical depths refer to the velocity at the photosphere,  $15,000 \text{ km s}^{-1}$ .) In spite of having a considerable number of free parameters at our disposal, we are left with two serious discrepancies: the observed absorption minima near  $4300$  and  $4700 \text{ \AA}$  are not accounted for. (The discrepancy from  $3900 \text{ \AA}$  to  $4200 \text{ \AA}$  is not very troubling because SYNOW spectra often are underblanketed in the blue due to the lack of weak lines of unused ions.) We have been unable to remove the  $4300$  and  $4700 \text{ \AA}$  discrepancies by introducing any additional ions that would be plausible under these circumstances, according to the LTE calculations of Hatano et al. (1999).

The lower panel of Figure 1 shows what we consider to be the most plausible way to improve the fit. The only difference in the synthetic spectrum is that we have introduced a high-velocity Fe II component, from  $22,000 \text{ km s}^{-1}$  to  $29,000 \text{ km s}^{-1}$ . Note that this leaves a gap from  $17,000$  to  $22,000$  where the adopted Fe II optical depth is zero. Introducing the high-velocity component of Fe II accounts rather well for the  $4300$  and  $4700 \text{ \AA}$  absorptions (and it also improves the  $3900\text{--}4200 \text{ \AA}$  region).

For later reference we mention here that the apparent blue edge of the Ca II H&K absorption feature reaches to 40,000 km s<sup>-1</sup> (or 32,000 km s<sup>-1</sup> if formed by Si II  $\lambda$ 3858, or 27,000 km s<sup>-1</sup> if formed by Si III  $\lambda$ 3801); the blue edge of the red Si II feature formed by  $\lambda$ 6355 reaches to 25,000 km s<sup>-1</sup>.

#### 4.2. Eight and Two Days Before Maximum

In the upper panel of Figure 2 an observed –8 day spectrum is compared with a synthetic spectrum that has  $v_{phot} = 12,000$  km s<sup>-1</sup>. The other fitting parameters are listed in Table 2. Here, we use only a weak contribution from high-velocity Fe II, from 20,000 to 25,000 km s<sup>-1</sup>, and without it the fit would be only slightly worse. But now, in this synthetic spectrum, we use two components of Ca II. A high-velocity (25,000 to 40,000 km s<sup>-1</sup>) component of Ca II is the only plausible way we have found to account for the observed absorption from 7800 to 8000 Å. This feature is present in other spectra at similar epochs and therefore is definitely a real feature; we attribute it to the Ca II infrared triplet, forming in the high-velocity component.

In the lower panel of Figure 2 an observed –2 day spectrum is compared with a synthetic spectrum that has  $v_{phot} = 11,000$  km s<sup>-1</sup>. The other fitting parameters are listed in Table 3. In the synthetic spectrum we still are using two components of Ca II, one extending from the photosphere to 16,000 km s<sup>-1</sup>, and the other from 20,000 to 23,000 km s<sup>-1</sup>. This two-component calcium leads to good agreement with the observed “split” of the Ca II H&K feature. Other ways to account for the H&K split might be to invoke Si II  $\lambda$ 3858 or Si III  $\lambda$ 3801 (Kirshner et al. 1993; Höflich 1995; Nugent et al. 1997; Lentz et al. 1999) but at this epoch of SN 1994D we find that in LTE, at least, other Si II or Si III lines would have to be made too strong compared with the observations. Our main reason for preferring the two-component Ca II at this epoch, however, is that it can account for

the observed absorption near 8000 Å. (As we will discuss in a future paper, we find strong support for this interpretation in Figure 4 of Meikle & Hernandez (1999), which compares spectra of SNe 1981B, 1994D, and 1998bu. In SNe 1994D and 1998bu both the H&K and the infrared–triplet absorption features are split, while in SN 1981B neither is split.)

At present we have no explanation for the general difference between the levels of the observed and synthetic spectra from 6500 to 7900 Å, other than to note that we are inputting a simple blackbody continuum from the photosphere.

The inset in the lower panel of Figure 2 compares the observed spectrum near the 1.05  $\mu\text{m}$  IR absorption to a synthetic spectrum that is an extension of the optical synthetic spectrum. We see that at this epoch Mg II, with the same reference–line optical depth we use to fit the optical features, accounts nicely for the IR absorption. Thus we, like Wheeler et al. (1998), favor the Mg II identification for the infrared absorption. The inset also illustrates the possibility that O I may be affecting the spectrum near 1.08  $\mu\text{m}$ ; here, in order not to mutilate the Mg II feature, we have had to reduce the O I reference–line optical depth by a factor of three compared to the value we used for the optical spectrum, which we would have to attribute to NLTE effects.

### 4.3. Evolution of the Ca II H&K Feature

Figure 3 shows the evolution of the Ca II H&K feature. If, as we suspect, the whole profile at  $-12$  and  $-11$  days is dominated by Ca II, then *some* Ca II must be present throughout the interval 15,000 – 40,000  $\text{km s}^{-1}$ . At later times, from 21 to 74 days, the Ca II absorption forms only at velocities less than about 15,000  $\text{km s}^{-1}$ . (The weak absorption near 3650 Å is probably produced by an iron–peak ion rather than by Ca II.) However, between  $-9$  and  $-3$  days the profile undergoes a complex evolution. While the

highest-velocity absorption ( $> 22,000 \text{ km s}^{-1}$ ) fades away, and the low-velocity absorption ( $< 15,000 \text{ km s}^{-1}$ ) develops, a dip appears near  $19,000 \text{ km s}^{-1}$  and a peak develops near  $16,000 \text{ km s}^{-1}$ . The  $19,000 \text{ km s}^{-1}$  dip is the bluer component of the split discussed above for  $-2$  days. As explained in the previous section we suspect that the  $19,000 \text{ km s}^{-1}$  minimum is caused by Ca II (rather than by Si II or Si III) mainly because of the Ca II IR triplet. If this is so, then at these phases there must be a local minimum in the Ca II radial optical depth profile around  $16,000 \text{ km s}^{-1}$ . This is not necessarily inconsistent with the smooth H&K profiles at  $-12$  and  $-11$  days if at those early times the line optical depth was high throughout the  $15,000$  to  $40,000 \text{ km s}^{-1}$  interval.

## 5. Discussion

Assuming that our line identifications are correct, what is the cause of this complex spectral behavior? One part that seems clear is that all of the matter detected at velocities lower than about  $16,000 \text{ km s}^{-1}$  represents freshly synthesized material. And the highest-velocity matter — calcium up to  $40,000 \text{ km s}^{-1}$ , iron up to  $30,000 \text{ km s}^{-1}$ , and silicon up to  $25,000 \text{ km s}^{-1}$  (from the blue edge of the red Si II line), is likely to be primordial. This would be consistent with the predictions of Hatano et al. (1999), for a composition in which hydrogen and helium have been burned to carbon and oxygen and the mass fractions of heavier elements are just solar; in this case the ions that are most likely to produce detectable spectral features from the primordial abundances are just the three that do appear to be detected at high velocity — Ca II, Fe II, and Si II.

However, what is the cause of the optical-depth minima of Ca II and Fe II, somewhere around  $16,000 \text{ km s}^{-1}$ ? One possibility is that the ionization and excitation structure is such that the Ca II and Fe II lines, which decrease in strength with increasing temperature, have optical-depth minima around  $16,000 \text{ km s}^{-1}$ . Some weak support for this comes

from the fact that in the  $-12$  day spectrum we found Fe III lines, forming just between 19,000 and 20,000 km s $^{-1}$ , to be helpful in fitting the spectrum. In addition, in detailed atmosphere calculations for model W7 with various primordial metallicities, Lentz et al. (1999) find a temperature maximum for low metallicity (see also Höflich 1995). SN 1994D had an unusually negative value of  $U - B$  for a Type Ia supernova, which could be an indication of low metallicity.

Another possibility is that there is a local minimum in the radial density profile around 16,000 km s $^{-1}$ . Delayed–detonation models have smoothly decreasing densities in their outer layers, and deflagration models tend to have only low–amplitude density peaks and dips. Pulsating–detonation and tamped–detonation models have more pronounced density minima, but at least in published models they occur at velocities that are lower than 16,000 km s $^{-1}$  (Khoklov, Müller, & Höflich 1993).

A third possibility is a nuclear explanation. Detailed nucleosynthesis calculations in delayed–detonation models recently have been carried out by Iwamoto et al. (1999). As we will discuss more thoroughly in another paper, the composition structures of some of their models are generally consistent with most of the constraints that we have inferred for SN 1994D. In their model CS15DD1, for example, the fractional abundances of freshly synthesized silicon, sulfur, calcium, and iron begin to drop sharply above about 15,000 km s $^{-1}$ , consistent with what we find for SN 1994D. It is interesting that in CS15DD1 the fractional abundances of sulfur and argon have pronounced minima around 16,000 km s $^{-1}$ . Perhaps a delayed–detonation model could be constructed to have a minimum in the fractional abundance of freshly synthesized calcium around 16,000 km s $^{-1}$ , although it seems unlikely that such could be the case for iron. It should be noted that the synthesis of calcium and iron depends on the initial metallicity (Höflich et al. 1998). Iwamoto et al. did not include primordial metals in their models. Perhaps when primordial metals are



included, models will be found in which both calcium and iron have fractional abundance minima near  $16,000 \text{ km s}^{-1}$ , if nuclear reactions can reduce the levels of calcium and iron below the primordial levels at this velocity. These possibilities appear to be plausible and they are being investigated (F.–K. Thielemann, personal communication).

## 6. Conclusion

Based on our interpretation of the pre–maximum–brightness spectra of SN 1994D, it appears that given high–quality spectra obtained at sufficiently early times, it should be possible to probe the primordial composition of the SN Ia progenitor (see also Lentz et al. 1999). This will be important in connection with using high–redshift SNe Ia as distance indicators for cosmology (Branch 1998; Perlmutter et al. 1998; Riess et al. 1998), for testing the predicted dependence of hydrodynamical models on primordial composition (Höflich et al. 1998), and for testing the prediction that low metallicity inhibits the ability of white dwarfs to produce SNe Ia (Kobayashi et al. 1998). It also appears that early spectra of SNe Ia can be used to place useful constraints on the nature of the nuclear burning front in the outer layers of the ejected matter.

Transforming the present somewhat qualitative indications into reliable quantitative results will require (1) further parameterized spectrum calculations, as part of a detailed comparative study of early–time spectra of SNe Ia (Hatano et al., in preparation); (2) detailed NLTE calculations for SN Ia hydrodynamical models before the time of maximum light (Nugent et al. 1997; Höflich et al. 1998; Lentz et al. 1999); (3) further detailed calculations of nucleosynthesis in parameterized hydrodynamical explosion models (Iwamoto et al. 1999); and (4) many more high–quality observed spectra of SNe Ia before the time of maximum brightness.

We are grateful to Dean Richardson and Thomas Vaughan for assistance, to Friedel Thielemann for discussions of nucleosynthesis in hydrodynamical models, and to Ferdinando Patat and Peter Meikle for making their observed spectra available in electronic form. This work was supported by NSF grants AST-9417102 to D.B., AST-9731450 to E.B., AST-9417213 to A.V.F., and NASA grant NAG5-3505 to E.B. and D.B.

## REFERENCES

- Branch, D. 1998, *ARAA*, 36, 17
- Filippenko, A. V. 1997a, in *Thermonuclear Supernovae*, ed. P. Ruiz–Lapuente, R. Canal, & J. Isern, Kluwer, Dordrecht, p. 1
- Filippenko, A. V. 1997b, *ARA&A*, 35, 309
- Fisher, A. 1999, Ph.D thesis, University of Oklahoma
- Fisher, A., Branch, D., Nugent, P., & Baron, E. 1997, *ApJ*, 481, L89
- Fisher, A., Branch, D., Hatano, K., & Baron, E. 1999, *MNRAS*, 304, 67
- Hatano, K., Branch, D., Fisher, A., Millard, J., & Baron, E. 1999, *ApJS*, in press  
(astro-ph/9809236)
- Höflich, P. 1995, *ApJ*, 443, 89
- Höflich, P., Wheeler, J. C., & Thielemann, F.–K. 1998, *ApJ*, 495, 617
- Iwamoto, K., Brachwitz, F., Nomoto, K., Kishimoto, N., Hix, W. R., & Thielemann, F.–K. 1999, *ApJ*, submitted
- Khoklov, A., Müller, E., & Höflich, P. 1993, *A&A*, 270, 223
- Kirshner, R. P. et al. 1993, *ApJ*, 415, 589
- Kobayashi, C., Tsujimoto, T., Nomoto, K., Hachisu, I., & Kato, M. 1998, *ApJ*, 503, L155
- Lentz, E. J., Baron, E., Branch, D., Hauschildt, P. H., & Nugent, P. E. 1999, *ApJ*, submitted
- Mazzali, P. A., & Lucy, L. B. 1998, *MNRAS*, 295, 428
- Meikle, W. P. S. et al. 1996, *MNRAS*, 281, 263
- Meikle, W. P. S. & Hernandez, M. 1999, *J. Ital. Astr. Soc.*, in press

- Millard, J. et al. 1999, ApJ, in press
- Nomoto, K., Thielemann, F.-K., & Yokoi 1984, ApJ, 286, 644
- Nugent, P., Baron, E., Branch, D. Fisher, A., & Hauschildt, P. H. 1997, ApJ, 485, 812
- Patat, F., Benetti, S., Cappellaro, E., Danziger, I. J., Della Valle, M., Mazzali, P. A., & Turatto, M. 1996, MNRAS, 278, 111
- Perlmutter, S. et al. 1999, ApJ, in press
- Richmond, M. W. et al. 1995, AJ, 109, 2121
- Riess, A. G. et al. 1998, AJ, 116, 1009
- Treffers, R. R., Filippenko, A. V., Van Dyk, S. D., & Richmond, M. W. 1994, IAU Circ. No. 5946
- Vacca, W. D., & Leibundgut, B. 1996, ApJ, 471, L37
- Wheeler, J. C., Höflich, P., Harkness, R. P., & Spyromilio, J. 1998, ApJ, 496, 908

Fig. 1.— A  $-12$  day observed spectrum in  $F_\lambda$  (Filippenko 1997a,b) is compared with synthetic spectra that have  $v_{phot} = 15,000 \text{ km s}^{-1}$ . In the upper panel, ions that contribute features in the synthetic spectrum are labeled. In the lower panel a second, high-velocity component of Fe II is added. In this and subsequent figures, the spectra are in the SN 1994D rest frame.

Fig. 2.— In the upper panel, a  $-8$  day observed spectrum in  $F_\nu$  (Patat et al. 1996) is compared to a synthetic spectrum that has  $v_{phot} = 12,000 \text{ km s}^{-1}$ . In the lower panel, a  $-2$  day observed spectrum in  $F_\nu$  (Patat et al. 1996) is compared to a synthetic spectrum that has  $v_{phot} = 11,000 \text{ km s}^{-1}$ . In the inset of the lower panel a  $-2$  day near-infrared spectrum (Meikle et al. 1996) is compared with an extension of the optical synthetic spectrum, except that the O I reference-line optical depth has been reduced by a factor of three. (The narrow spike near  $1.13 \mu\text{m}$  is an artifact.)

Fig. 3.— Observed spectra in the region of the Ca II H&K feature (Filippenko 1997a,b). The solid vertical line corresponds to  $3945 \text{ \AA}$  (the  $gf$ -weighted rest wavelength of Ca II H&K) and the dashed vertical lines are blueshifted by  $10,000$ ,  $20,000$ , and  $30,000 \text{ km s}^{-1}$ .